Pramana – J. Phys. (2019) 93:8
https://doi.org/10.1007/s12043-019-1766-7

Monte Carlo simulation of charge transport in disordered organic systems using buffer lattice at the boundary

S RAJ MOHAN[1,*], MANORANJAN P SINGH[2,3] and M P JOSHI[1,3]

[1]Laser Materials Processing Division, Raja Ramanna Centre for Advanced Technology, Indore 452 013, India
[2]Theory and Simulation Lab, Raja Ramanna Centre for Advanced Technology, Indore 452 013, India
[3]Homi Bhabha National Institute, Training School Complex, Anushakti Nagar, Mumbai 400 094, India
*Corresponding author. E-mail: raj@rrcat.gov.in; rajmho@gmail.com

MS received 1 July 2018; revised 12 December 2018; accepted 17 December 2018;
published online 4 May 2019

Abstract. In this paper, we present an alternative method for simulating the charge transport in disordered organic materials by using a buffer lattice at the boundary. This method does not require careful tracking of the carrier's hopping pattern across boundaries. The suitability of this method is established by reproducing the field dependence of mobility, carrier relaxation and carrier diffusion in disordered organic systems obtained by simulating the charge transport in a lattice without implementing any boundary conditions along the electric field direction. The significance of the buffer lattice is emphasised by simulating the field dependence of mobility without using a buffer lattice, which results in negative field dependence of mobility (NFDM) at low field regime due to the extra bias the carrier gains from the neglected hops at the boundaries along the direction of the electric field.

Keywords. Disordered system; charge transport; Monte Carlo simulation; negative field dependence of mobility; periodic boundary condition; buffer lattice.

PACS Nos 72.80.Le; 72.20.Ee; 71.55.Jv; 02.70.−c; 02.70.Uu

1. Introduction

Gaussian disorder model (GDM) [1–4] is a widely used model for explaining the charge transport behaviour observed in disordered organic systems. According to GDM, the charge transport in disordered organic materials occurs by hopping among transport sites that are subjected to energetic and positional disorders [1–4]. As the model assumes Gaussian density of states [1–4], a complete analytical solution of the hopping transport is difficult, especially in 3D. Hence, the predictions of the GDM were made on the basis of Monte Carlo simulation of hopping charge transport [1–4]. The Monte Carlo simulation is considered as an idealised experiment with which one can study the charge transport in disordered systems as a function of several parameters [1–5]. The Monte Carlo simulation along with quantum chemical calculation and molecular dynamic simulation is extensively used for investigating material-specific charge transport properties [6].

Generally, charge transport is simulated for thin films with thickness of a few microns. This is to make sure that the carrier has attained a dynamic equilibrium during the transit and also to have a better comparison with the experiments, such as time-of-flight (TOF), that are generally performed on micron-sized thick samples [1–4]. Periodic boundary condition (PBC) is well established and frequently used [7–12] to simulate the charge transport in micron-thick thin films. PBC is a set of boundary conditions that are used to simulate the properties of bulk system by simulating a part of it [13]. In principle, the PBC generates an infinitely large system with the help of a smaller array that represents only a part of the bulk system, with the assumption that the small array will replicate periodically in all the three directions to form the bulk system. In PBC, when a carrier moves out through one of the boundaries, a similar carrier is injected in through the opposite boundary [13]. In this process, the carrier's energy and the other Cartesian coordinates, other than the directions along which the PBC is applied, remain the same as those at the boundary. In essence, the advantage of using the PBC is that the simulation can be performed on a sample length of several microns using an array of smaller size while at the same time reproducing the results obtained when simulated without using the PBC. If PBC is not used,

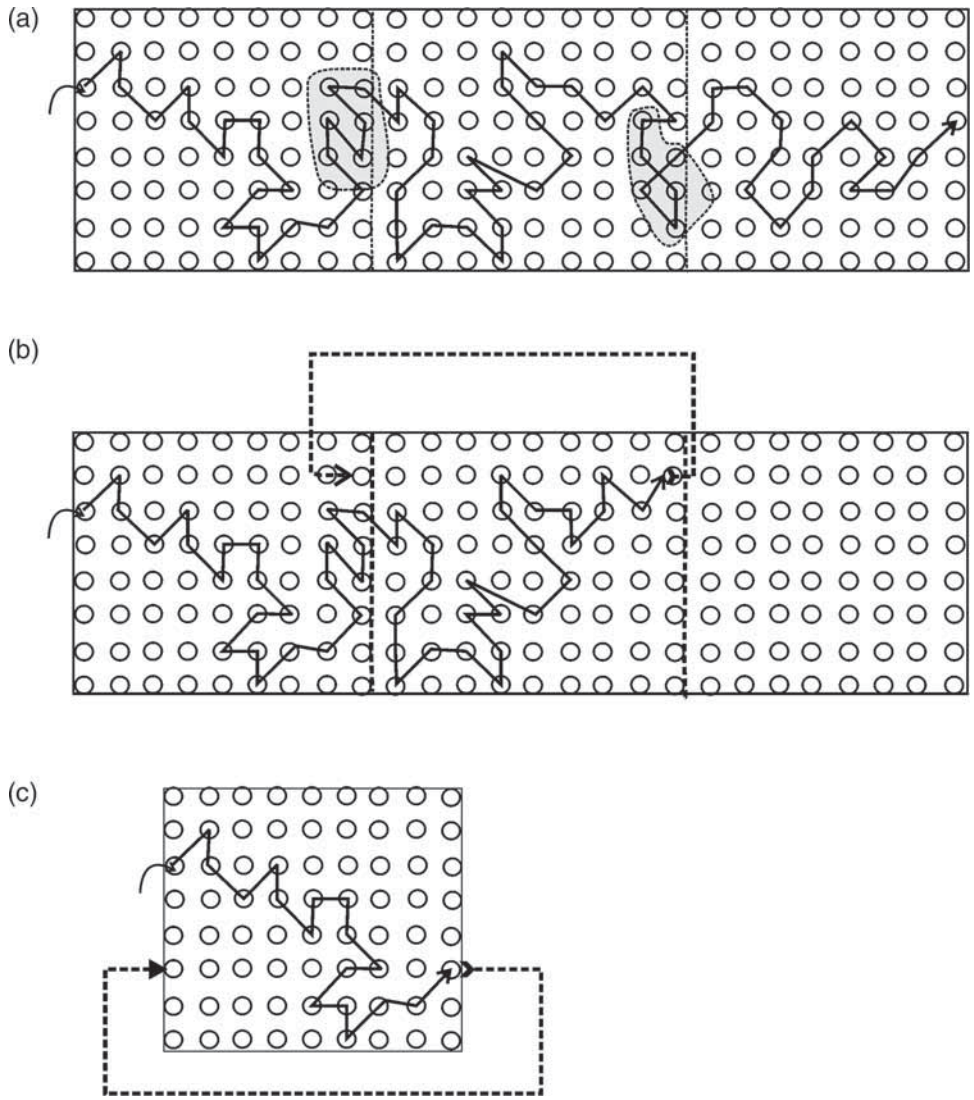

Figure 1. Schematic diagram showing a typical hopping motion of the carrier inside the lattice for (**a**) Case 1, (**b**) Case 2 and (**c**) Case 3. Shaded region in (**a**) shows the hops that are neglected at the boundaries when Case 3 is implemented.

then an array of bigger sizes, in all the three Cartesian directions, is required, which demands large computational resources.

A meticulous implementation of the carrier's hopping pattern across the boundaries is indispensable for implementing PBC. All the backward and forward hops across the boundaries must be taken care of. Otherwise, serious artefacts may arise. In this work, we propose an alternative method of implementing the simulation with the help of buffer lattice region at the boundaries. Buffer regions have been commonly used for simulations in other areas of research [14], but the use of buffer lattice in the Monte Carlo simulation of charge transport in disordered organic system [1–4] has not been reported earlier. In this method, when the carrier reaches a defined final boundary plane in the field direction, then the carrier is taken to another defined plane of the lattice in the opposite direction, where the carrier gets a buffer lattice region. In the buffer lattice region, the carrier is allowed to perform all the hopping processes that it would have made in the absence of a boundary. This method does not require the stringent tracking of a carrier's hopping pattern. The accuracy of this method is established by reproducing various charge transport properties of the disordered organic systems obtained by simulating the charge transport, without implementing PBC along the field direction, in a lattice array whose size along the field direction is equal to the full length of the sample. In order to emphasise the role of the buffer lattice, the field dependence of mobility is simulated without using the buffer lattice along the field direction and the data are compared with the one

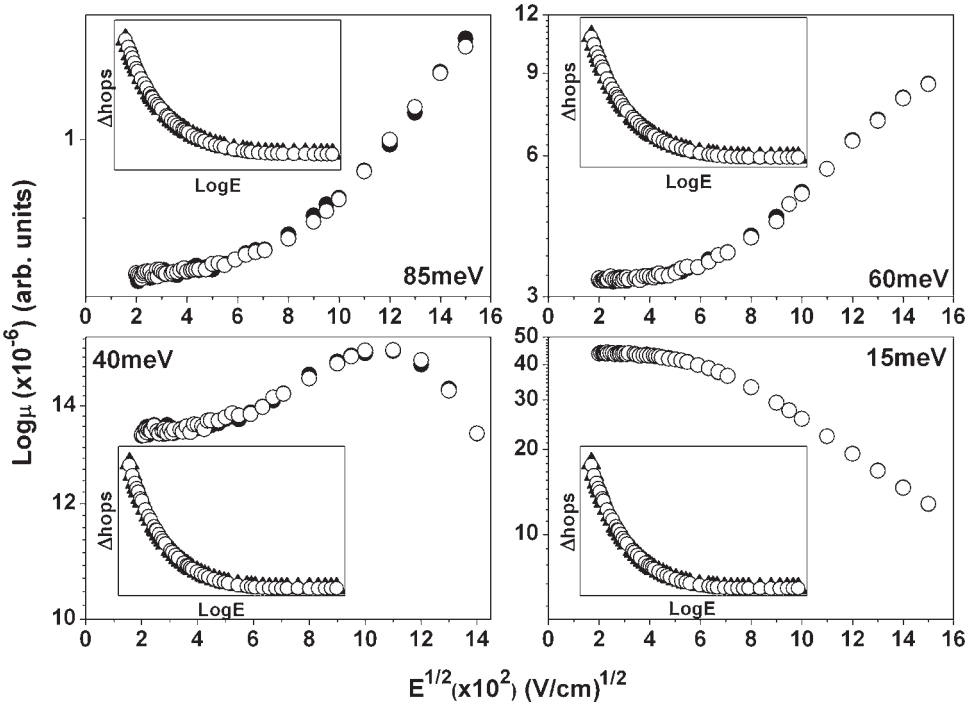

Figure 2. Comparison of the field dependence of mobility simulated for Case 1 (●) and Case 2 (○). Inset shows the comparison of total number of hops made by the carrier in Case 1 (▲) and Case 2 (○).

obtained by full sample length simulation (FLS). The discrepancy is observed mainly at the low field regime. At low field regime, the field dependence of mobility, when simulated without buffer lattice and with zero positional disorder, shows negative field dependence of mobility (NFDM) for all values of energetic disorder. But, by FLS, a clear saturation of mobility with field is observed at low field regime. In the absence of buffer lattice, some of the hops that the carrier may make in the absence of such a boundary are neglected. These neglected hops give an extra bias to the carrier, resulting in the enhanced mobility that leads to NFDM. Thus, this study also highlights the importance of the flawless implementation of the carrier's hopping pattern at the boundaries, while implementing PBC, failure of which results in a serious artefact that can mislead the interpretation and the modelling of charge transport in disordered organic systems.

2. Details of Monte Carlo simulation

The Monte Carlo simulation is based on the commonly used algorithm reported by Schönherr *et al* [15]. A 3D array is considered as the lattice with size 70×70 along x and y directions. Along the z direction, i.e. the direction of the applied field, various array sizes are used to implement different simulation approaches adopted for covering the required sample thickness. Simulation is always performed for a sample length of 4 μm along the field direction with lattice constant $a = 6$ Å [1]. In all, the following approaches are considered:

Case 1 (FLS): In this case, a lattice of size $70 \times 70 \times 7000$ along x, y and z directions is used for simulation. Simulation is performed without using PBC along the z direction (figure 1a), which requires array of bigger size. However, PBC is implemented along x and y directions. In this case, the carrier does not see any boundary along the z direction till it covers the required sample thickness.

Case 2: This is an alternative method for simulating the charge transport (figure 1b) by using a buffer lattice at the boundaries. In this case, a lattice of size $70 \times 70 \times 150$ along x, y and z directions is used. The carrier injected into $z = 1$ plane is allowed to move in the direction of the applied electric field. The carrier is taken into $z = 70$th plane once it crosses $z = 140$th plane while maintaining the same carrier energy and x/y coordinates. Therefore, the lattice region up to $z = 69$ acts as a buffer lattice for the carrier taken to the 70th plane. Around $z = 70$th plane, the carrier performs all the hops that it would have made in the absence of a boundary. Similarly, the carrier reaches any boundary along x and y directions and is taken to the middle of the plane defined by the current value of z with the same energy. This approach considers all the carrier hops at

the boundaries to be perpendicular to the z direction because the carrier is allowed to execute the necessary hops inside the lattice. Use of the buffer lattice region along the x and y directions similar to the z direction is also possible. However, this requires a bigger array for providing buffer lattices around the boundaries along the x and y directions. In general, this method is an alternative method for simulating the charge transport in disordered organic systems with reasonable computational resources. Case 2 requires less computational resources than Case 1. Moreover, this method does not require the careful tracking of the carrier's hopping pattern.

Case 3: In this case, a lattice of size $70 \times 70 \times 70$ along x, y and z directions is used for simulation (figure 1c). This method of simulation and analysis of the data emphasises and illustrates the role of buffer lattice adopted in Case 2, as described earlier. In this case, PBC is implemented only along x and y directions. Along the applied field direction, the carrier is taken to the first plane ($z = 1$) once the carrier reaches 70th plane, keeping the carrier energy and the other coordinates the same as those at the boundary. In this method, the carrier taken to the first plane cannot perform a backward hop at the boundary along the field direction, i.e. carrier taken to the first plane proceeds in the field direction similar to a carrier injected initially but with the relaxed energy it has attained during the hopping process. Hence, some of the hops that the carrier would have made in the absence of boundaries, which it encounters in the process of transit along the z directions, are neglected. In Case 2, the carrier performs these neglected hops in the buffer region. Hence, the data obtained by this method not only emphasise the role of buffer lattice in Case 2 but also highlight the possible artefact that can arise if the carrier's hopping pattern across boundaries is not properly taken care of while implementing the PBC. In Case 3, if PBC is also applied along the z direction, then this method becomes similar to the conventional simulation methodology with PBC along all the directions and the data produced are similar to the other two cases (data not shown).

In each of the aforementioned cases, the hopping of the carrier between sites i and j is decided by the probability that a carrier jumps from the present site i to another site j around and within a cube of size $7 \times 7 \times 7$ (343 sites) [11]. Therefore, in Case 2, the buffer lattice between $z = 140$ and 150 eases the probability calculation for carrier hopping (within $7 \times 7 \times 7$ sites around the carrier) at the boundary, instead of dealing with the sites at the opposite boundaries. Each node of the array is considered as a localised transport site with uncorrelated site energy. The uncorrelated site energies of the lattice are

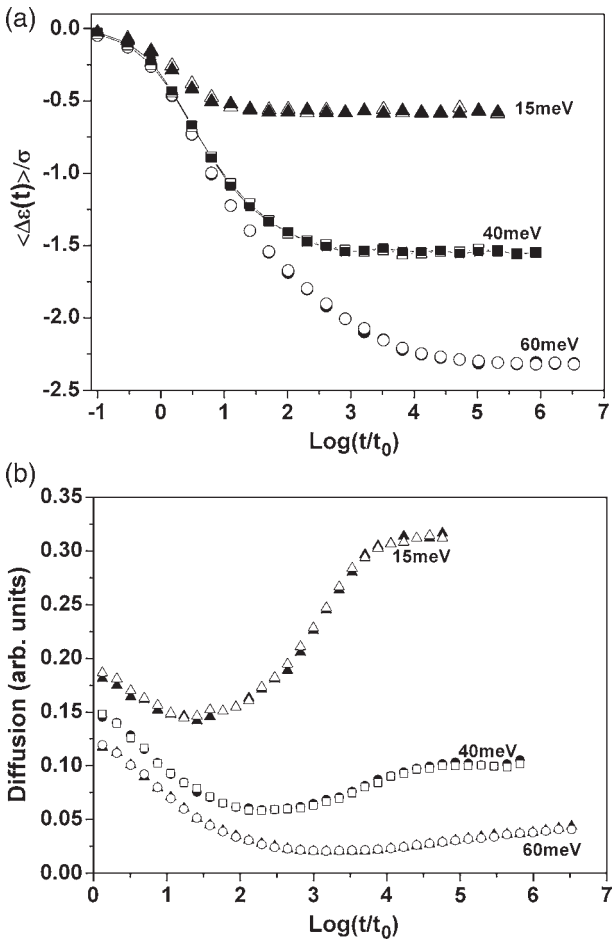

Figure 3. Comparison of (**a**) relaxation and (**b**) diffusion of carriers simulated using Cases 1 and 2. Open symbols show the data obtained using Case 2. Simulation is carried out for $E = 7.5 \times 10^4$ V/cm and $T = 300$ K.

taken randomly from a Gaussian distribution with a known standard deviation (σ), which is the measure of the energetic disorder of the sample. Simulations are performed for various values of σ and electric field strengths at 300 K. Throughout the simulation, the positional disorder is neglected ($\Sigma = 0$). This is to avoid the huge computational time required for simulating the charge transport with non-zero positional disorder. Moreover, the outcome of this study can be clearly shown even without positional disorder. The carrier hopping in this energetically disordered lattice is governed by the Miller–Abrahams equation [16,17]. The Miller–Abrahams equation for the jump rate (ν_{ij}) of the charge carrier from the site i to site j is given by

$$\nu_{ij} = \nu_0 \exp\left(-2\gamma a \frac{\Delta R_{ij}}{a}\right) \times \begin{pmatrix} \exp\left(-\dfrac{\varepsilon'_j - \varepsilon'_i}{kT}\right), & \varepsilon'_j > \varepsilon'_i \\ 1, & \varepsilon'_i > \varepsilon'_j \end{pmatrix}, \quad (1)$$

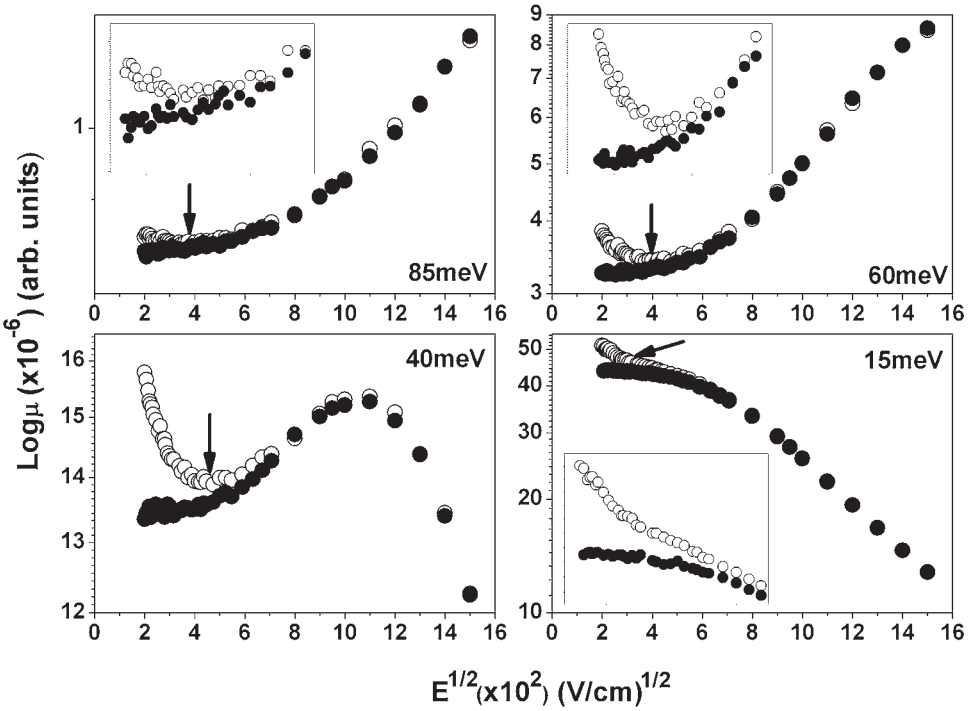

Figure 4. Comparison of field dependence of mobility for various values of disorder for Case 3 (○) and Case 1 (●). Arrow shows the minima of mobility occurred at low field regime in Case 3. Enlarged view of the low field regime for the respective cases is shown in the inset.

where ε_i' and ε_j' are the effective energies of the sites i and j including the electrostatic energy, a is the inter-site distance, $\Delta R_{ij} = |R_i - R_j|$ is the distance between sites i and j,k is the Boltzmann constant, T is the temperature in kelvin and $2\gamma a$ is the wave function overlap parameter that controls the electronic exchange interaction between the sites. Throughout the simulation, we took $2\gamma a = 10$ [1,15]. Transit time of a carrier is calculated by adding all the hopping times and averaging over a few hundreds of carriers. The mobility is calculated using drift mobility equation. The electric field range ($>10^4$ V/cm) over which the simulations are carried out is higher, and hence, the diffusion cannot dominate the charge transport [18,19]. Thus, the use of drift mobility equation is justified.

3. Results and discussion

Figure 2 shows the comparison of the field dependence of mobility, for various values of energetic disorder, obtained from Cases 1 and 2. For both the cases, the field dependence of mobility for all the values of energetic disorder under study is similar and superimposes on each other. Inset shows the total number of hops that the carriers take for traversing the required sample length. There is no remarkable difference in the total number of hops made by the carrier in traversing the sample when simulated using Cases 1 and 2. In addition to the field dependence of mobility, other data such as relaxation, diffusion, etc. calculated using Case 2 are also identical to that obtained using Case 1. Figures 3a and 3b show the temporal changes in the mean energy and diffusion of carriers during the transit. Both the energy of the carriers and the diffusion have attained a steady-state value which confirms that in both the cases, the carrier has attained a dynamic equilibrium [20,21]. In both the cases, the temporal variation of mean energy and diffusion of the carrier occur in a similar manner and attain their respective steady-state values in the same time frame. This clearly shows that the charge transport in disordered organic system can be accurately simulated by using the buffer lattice at boundaries as in Case 2. Inside the buffer lattice, the carrier makes all the necessary hops that it would have made in the absence of such a boundary. Case 2 requires less computational space than Case 1. In addition, a precise following of the carrier's hopping pattern is also not necessary when simulation is carried out as in Case 2.

In order to emphasise the role of buffer lattice in Case 2, the field dependence of mobility is also simulated without using the buffer lattice (Case 3) and compared with the data obtained using Case 1. The field dependence of mobility, for various values of energetic disorder, obtained from Cases 1 and 3 is shown in figure 4. For both the cases, the field dependence of mobility

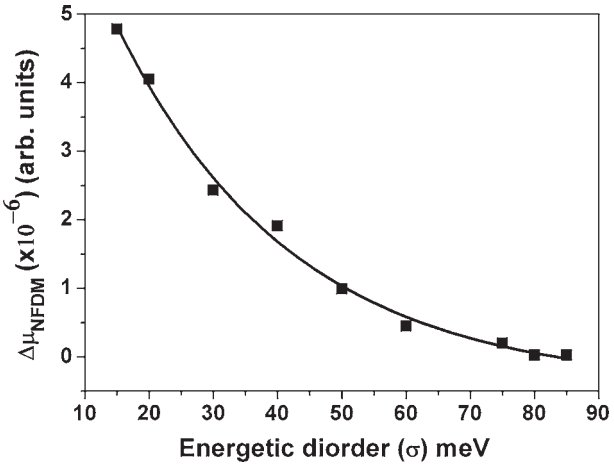

Figure 5. Variation in the strength of NFDM ($\Delta\mu_{\mathrm{NFDM}}$), observed in Case 3, with energetic disorder. Solid line is a guide to eye.

for all the values of energetic disorder under study is similar except at lower electric field strengths ($\sim<$ 3.6×10^5 V/cm). In Case 3, at lower electric field strengths, the mobility first decreases with an increase in the electric field, i.e. NFDM. The mobility attains a minimum value (indicated by arrows in figure 4) and then shows a positive field dependence given by $\ln \mu \propto E^{1/2}$ as predicted by GDM [1–4]. In Case 1, for all the values of energetic disorder, a clear saturation of mobility is observed at lower electric field strengths [1–4]. NFDM is observed in Case 3 without any positional disorder ($\Sigma = 0$). The strength of the observed NFDM becomes remarkable when the energetic disorder decreases, as shown in figure 5. The strength of NFDM ($\Delta\mu_{\mathrm{NFDM}}$) is assigned as the difference in mobility value for the lowest electric field strength under study and the observed minima of the mobility at low field regime. The origin of the difference in field dependence of mobility, at lower electric field strengths, between Cases 1 and 2 is explained subsequently.

Figure 6 shows the variation in the total number of hops with electric field, for various values of energetic disorder, executed by the carrier to cover the required sample length when simulated with Cases 1 and 3. At low electric field strengths, for all the values of energetic disorder, the total number of hops made by the carrier to cover the required sample length in Case 1 is higher than that in Case 3. The maximum difference in total number of hops (Δhops) occurs at lowest electric field strength (4×10^4 V/cm), which decreases as the electric field strength increases and becomes negligible at very high electric field strengths. As the value of the energetic disorder increases, the value of Δhops also increases (inset of figure 6). In Case 3, the neglected hops can certainly influence the charge transport, especially the transit time. It is confirmed through simulation that the charge carriers have attained dynamic equilibrium [20,21] while covering the required sample length (data not shown). The neglected hops provide an extra

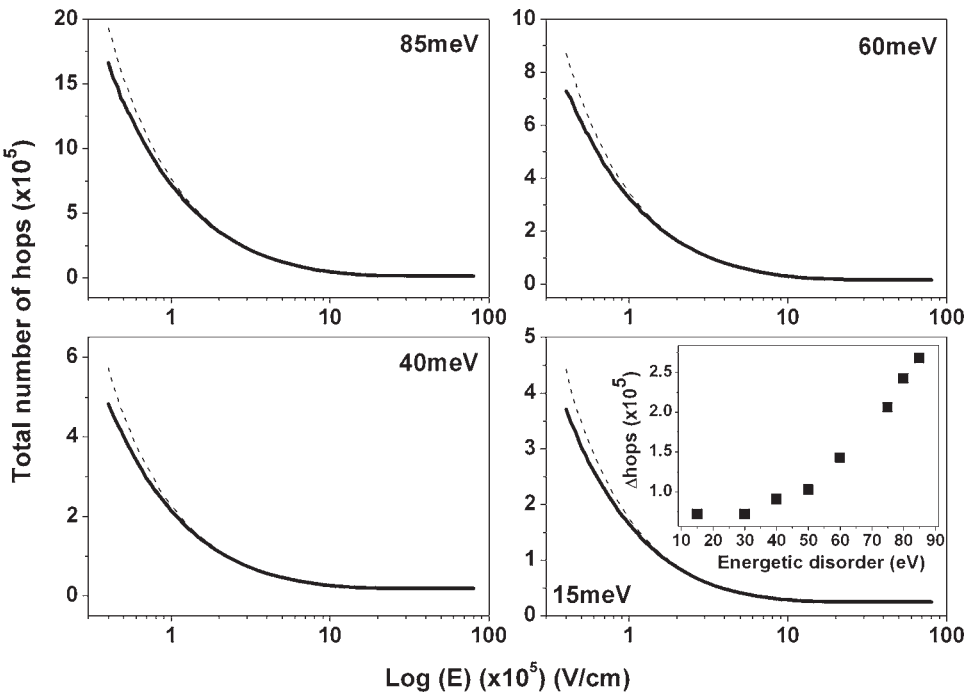

Figure 6. Field dependence of the total number of hops made by the carrier in two cases (Case 3 (solid line) and Case 1 (dashed line)) for various values of energetic disorder. Inset shows the dependence of difference in the total number of hops (Δhops), made by the carrier in Cases 1 and 3, with energetic disorder at 4×10^4 V/cm.

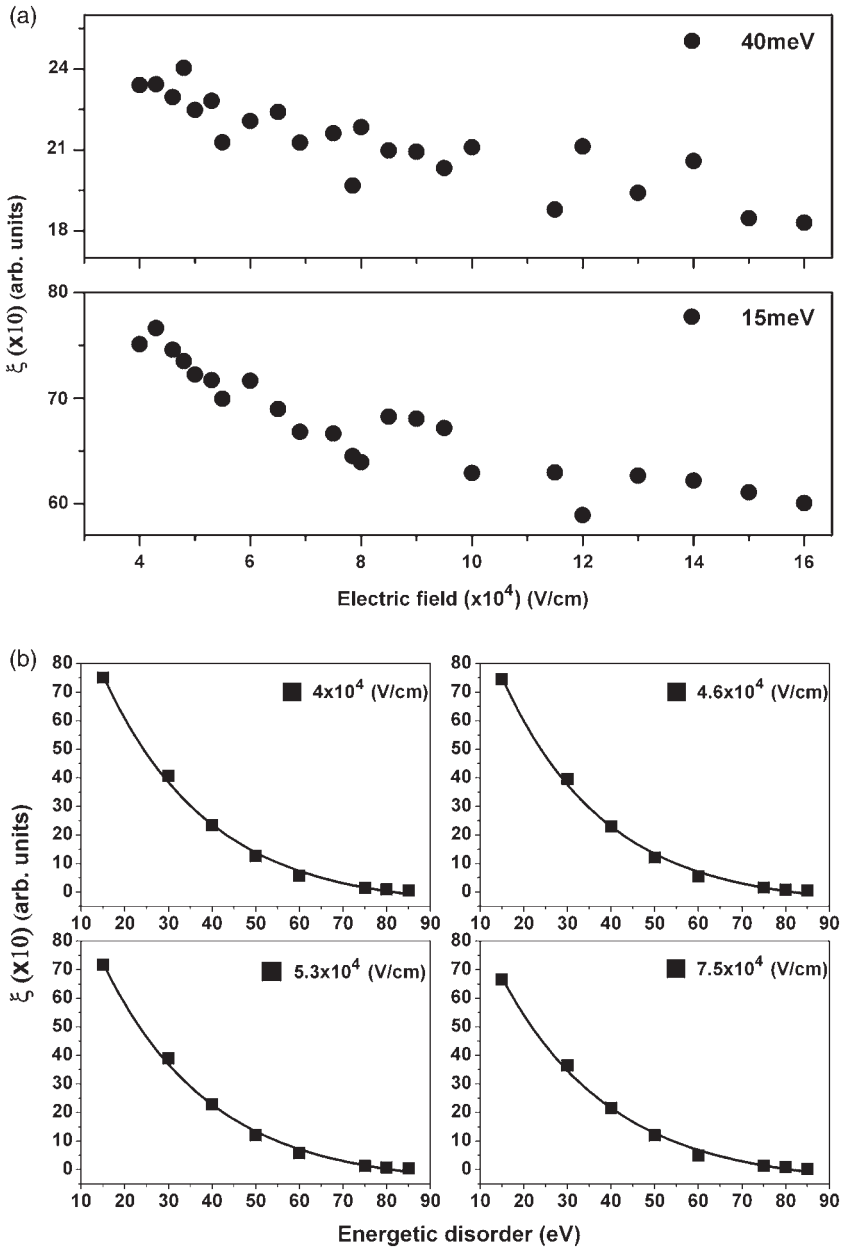

Figure 7. Variation of ξ (**a**) with electric field strength for the values of energetic disorder where reasonably strong NFDM is observed and (**b**) with energetic disorder for various values of electric fields at low field regime. Solid line is a guide to eye.

bias for the carrier to move in the applied field direction. The carrier covers the required sample length in less number of hops, which reduces the carrier transit time, thereby enhances the mobility. The maximum difference in transit time ($\Delta\tau$) between Cases 1 and 3 occurs at the highest value of Δhops. Thus, the strength of the NFDM in Case 3 is higher at lower electric field strength for any value of energetic disorder. As the electric field strength increases, Δhops and $\Delta\mu_{\mathrm{NFDM}}$ diminish concurrently. Similarly, for a constant electric field, the strength of the observed NFDM in Case 3 is expected to be higher at a higher value of energetic disorder. However, higher NFDM is observed at lower energetic disorder (figure 5). This is because the difference in mobility, for constant electric field and thickness, depends on the value of ξ instead on $\Delta\tau$ alone, as shown in the following equation:

$$\Delta\mu = \mu_2 - \mu_1 = \frac{L}{E}\left[\frac{1}{\tau_2} - \frac{1}{\tau_1}\right] = \frac{L}{E}\xi, \tag{2}$$

where L is the thickness of the sample, E is the applied electric field, $\xi = [\Delta\tau/\tau_2\tau_1]$ and $\Delta\tau$ is the difference in transit time between Cases 1 and 3, τ_2 is the transit time in Case 3 and τ_1 is the transit time in Case 1. Figures 7a and 7b show the variation of ξ as a function of

electric field and energetic disorder. The electric field is limited to the range where the value of $\Delta\tau$ is significant. For any value of energetic disorder, ξ decreases with an increase in the electric field strength (figure 7a). This supports the observed NFDM at low-field regime for all the values of energetic disorder. In addition, ξ decreases with an increase in energetic disorder (figure 7b). This suggests a higher $\Delta\mu_{\mathrm{NFDM}}$ for a lower value of energetic disorder and vice versa, as shown in figure 5. The aforementioned data clearly show an artefact that occurs at low electric field regime due to hops neglected when simulated using Case 3. Thus, the data obtained from Case 3 not only highlight the role of buffer lattice used in Case 2 but also assert the need for precise consideration of the carrier's hopping pattern across the boundaries while implementing the PBC for simulating charge transport in disordered organic materials.

Therefore, in Case 2, enough buffer array must be provided so that the carrier should not reach the $z = 1$ plane after it has taken to $z =$ 70th plane. After taking into $z =$ 70th plane, if the carrier hops back and touches $z = 1$ plane, then some hops may be neglected which in turn may result in NFDM. Hence, a sufficient buffer lattice must be provided for the wandering of the carrier around the $z =$ 70th plane. The dimension of the buffer lattice used in the study ($70 \times 70 \times 69$) is optimum for simulating the field dependence of mobility and other parameters for various energetic disorders under study.

4. Conclusion

In this study, a simulation method that excludes the use of PBC in the Monte Carlo simulation of charge transport in disordered organic systems is demonstrated. This method adopts the use of buffer lattices at the boundaries for the simulation. In this method, a carrier reaching one boundary plane is taken to another plane where the carrier is provided with a buffer lattice region. Inside the buffer lattice region, the carrier makes all the necessary hops that it would have made in the absence of a boundary. The importance of buffer lattice is emphasised by simulating the field dependence of mobility without using a buffer lattice, which results in NFDM at low field regime. The observed NFDM is due to the extra bias the carrier gains from the neglected hops at the boundaries in the absence of a buffer lattice region.

References

[1] H Bässler, *Phys. Status Solidi B* **175**, 15 (1993)
S V Noikov and A V Vanikov, *J. Phys. Chem. C* **113**, 2532 (2009)
[2] P M Borsenberger, L Pautmeier and H Bässler, *J. Chem. Phys.* **94**, 5447 (1991)
[3] L Pautmeier, R Richert and H Bässler *Synth. Met.* **37**, 271 (1990)
Y N Gartsetin and E M Conwell, *Chem. Phys. Lett.* **245**, 351 (1995)
[4] P M Borsenberger and D S Weiss, *Organic photoreceptors for xerography* (Marcel Dekker, New York, 1998)
[5] M Bahrami and E Mohajerani, *J. Comput. Electron.* **15**, 672 (2016)
[6] C Yao, Y Yang, L Li, M Bo, C Peng and J Wang, *J. Mater. Chem. C* **6**, 6146 (2018)
C Yao, C Peng, Y Yang, L Li, M Bo, C Peng and J Wang, *J. Phys. Chem. C* **22**, 22273 (2018)
[7] R Richert, L Pautmeier and H Bassler, *Phys. Rev. Lett.* **63**, 547 (1989)
[8] S V Rakhmanova and E M Conwell, *Appl. Phys. Lett.* **76**, 3822 (2000)
[9] B Hartenstein, H Bässler, S Heun, P Borsenberger, M Van der Auweraer and F C De Schryyer, *Chem. Phys.* **191**, 321 (1995)
[10] J Zhou, Y C Zhou, X D Gao, C Q Wu, X M Ding and X Y Hou, *J. Phys. D* **42**, 035103 (2009)
[11] S Raj Mohan, M P Joshi and M P Singh, *Org. Electron.* **9**, 355 (2008)
[12] S Raj Mohan, M P Joshi and M P Singh, *Chem. Phys. Lett.* **470**, 279 (2009)
[13] H Gould and J Tobochnik, *An introduction to computer simulation methods: Application to physical systems* (Addison-Wesley Publishing Company, New York, 1988)
[14] W F van Gunsteren and H J C Berendsen, *Angew. Chem. Int. Ed. Engl.* **29**, 992 (1990)
[15] G Schönherr, H Bässler and M Silver, *Philos. Mag.* **44**, 47 (1981)
S Raj Mohan, M P Singh and M P Joshi, *J. Phys. Chem. C* **116**, 2555 (2012)
[16] A Miller and E Abrahams, *Phys. Rev. B* **120**, 745 (1960)
[17] I Naik, S Handsa and A K Rastogi, *Pramana – J. Phys.* **86**, 127 (2016)
[18] I I Fishchuk, A Kadashchuk, H Bässler and M Abkowitz, *Phys. Rev. B* **70**, 245212 (2004)
[19] H Cordes, S D Baranovski, K Kohary, P Thomas, S Yamasaki, F Hensel and J H Wendorff, *Phys. Rev. B* **63**, 094201 (2000)
[20] B Movaghar, M Grunewald, B Ries, H Bässler and D Wrutz, *Phys. Rev. B* **33**, 5545 (1986)
[21] S Raj Mohan, M P Joshi and M P Singh, *Org. Electron.* **11**, 1642 (2010)